Inorganic Chemistry

Article

pubs.acs.org/IC

Electronic Spectra and Excited States of Neptunyl and Its $[NpO_2Cl_4]^{2-}$ Complex

Jing Su, W. H. E. Schwarz,[†] and Jun Li*

Department of Chemistry & Laboratory of Organic Optoelectronics and Molecular Engineering of the Ministry of Education, Tsinghua University, Beijing 100084, People's Republic of China

ABSTRACT: Electronic states and spectra of NpO_2^{2+} and $NpO_2Cl_4^{2-}$ with a Np $5f^1$ ground-state configuration, related to low-lying 5f−5f and ligand-to-metal charge-transfer (CT) transitions, are investigated, using restricted-active-space perturbation theory (RASPT2) with spin−orbit coupling. Restrictions on the antibonding orbital occupations have little influence on the 5f−5f transition energies, but an important impact on the CT states with an open bonding orbital shell. The present calculations provide significant improvement over previous literature results. The assignment of the experimental electronic spectra of $Cs_2NpO_2Cl_4$ is refined, based on our calculations of $NpO_2Cl_4^{2-}$. Assignments on the basis of bare NpO_2^{2+} are less reliable, since the equatorial Cl ligands perturb the excited-state energies considerably. Calculated changes of the Np−O bond lengths are in agreement with the observed short symmetric-stretching progressions in the f−f spectra and longer progressions in the CT spectra of neptunyl. A possible luminescence spectrum of the lowest quartet CT state is predicted.

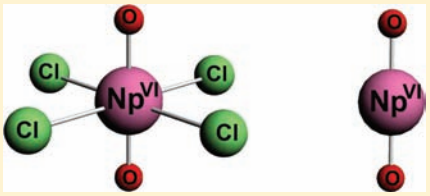

1. INTRODUCTION

The radioactive neptunyl (NpO_2^{2+}) and its reduced NpO_2^{+} species pose a significant challenge for the separation of spent nuclear fuel, for the safe disposal of nuclear waste, and for advanced nuclear fuel cycles. Prevalent radioisotope ^{237}Np is one of the most troublesome isotopes in nuclear waste. It has a half-life of 2.14×10^6 years, thereby constituting a major issue. Thus, understanding the coordination chemistry and the spectroscopy of neptunyl compounds is critical for nuclear waste management.[1]

Electronic structures of actinoid compounds are rather difficult to characterize, largely because of the number of multiplets and the high density of states common to open 5f-shell species. Compounds containing NpO_2^{2+} are particularly convenient targets of study, because they have reasonable chemical stability for experimental work while offering the simplest electronic structure, because of the presence of only a single 5f electron in the ground state. While the absorption and emission spectra of $5f^0$ uranyl (UO_2^{2+}, $D_{\infty h}$ symmetry) compounds have been investigated in great detail,[2−6] the electronic structures of the subsequent actinoyl systems (sometimes named actinyl, although not meaning AcO_2^{q}), i.e., $AnO_2^{2+/1+}$ for An = Np, Pu, Am, etc., are much less understood, mainly because of the complexity arising from the open An 5f-shell and the strong spin−orbit (SO) coupling. As a first step toward the interpretation and understanding of the electronic structure and spectra of the more-complicated systems, neptunyl(VI) had come into the focus of both electronic spectroscopy and quantum chemical research.[7]

Experimentally, Denning and co-workers had already analyzed the single-crystal absorption spectra of the Cs salts of $NpO_2Cl_4^{2-}$ and $NpO_2(NO_3)_3^{-}$ at liquid helium temperature, up to 22×10^3 cm^{-1}, in quite good detail 30 years ago.[8,9] They observed well-defined 5f−5f ligand-field transitions below 12×10^3 cm^{-1}, and interlaced f−f and ligand-to-metal charge-transfer (LMCT) transitions above that value. More recently, Wilkerson reported the first example of f−f luminescence of neptunyl in the solid state at 75 K[10] and later also at room temperature.[11,12] Talbot-Eeckelaers et al. then published the first observation of neptunyl luminescence in solution.[13] The luminescence in both of these studies occurs in the short-wavelength near-infrared region of $(6−7) \times 10^3$ cm^{-1}.

Theoretical investigations of excited states of actinoid compounds are challenging. Early efforts include investigations with semiempirical ligand field theory[8,9,14] and also with density functional theory (DFT).[15,16] In general, DFT or time-dependent DFT results are relatively accurate for low-lying f−f excited doublet states of f^1 systems;[17] however, their performances are poor for LMCT or for f^n ($n \geq 2$) systems. Wave-function-based ab initio methods are usually needed to obtain more-reliable results. Matsika and Pitzer[18] initiated the ab initio theoretical investigation of the electronic spectra of bare NpO_2^{2+} (f^1) and NpO_2^{1+} (f^2) applying an SO coupled configuration interaction (CI) method. Concerning NpO_2^{2+}, the calculated f−f and charge transfer (CT) transitions of the bare neptunyl ion were compared to Denning's $Cs_2NpO_2Cl_4$ spectra. Recently, Infante et al.[19] calculated the f−f transitions with an intermediate Hamiltonian multireference Fock-space (IHFS) coupled cluster (CC) approach. They obtained excitation energies that were 0.2−0.4 eV higher than the values of Pitzer et al. for those excitations in the 1 eV range.

Absorption and luminescence spectroscopy are powerful analytical diagnostics for the chemical speciation of actinoid ions relevant to nuclear waste disposal and related environmental issues. Therefore, it is important to elucidate the electronic

Received: December 17, 2011
Published: February 23, 2012

dx.doi.org/10.1021/ic202712p | Inorg. Chem. 2012, 51, 3231−3238

structure and excited states of neptunyl complexes. We have recently investigated the vibration-resolved luminescence spectra of uranyl–glycine–water complexes in solution[20] and that of UO_2Cl_2 in an argon matrix.[21,22] SO-coupled ab initio approaches such as coupled clusters with single, double, and perturbative-triple substitutions (CCSD(T)) and complete-active-space multiconfiguration self-consistent field (CASSCF) with many-electron second-order perturbation-theory (CASPT2) have proven its strength in reproducing the experimental spectral shapes and refining the assignments.[21]

The purpose of the present paper is a theoretical analysis of the electronic transitions in bare NpO_2^{2+} and in ligated $NpO_2Cl_4^{2-}$, focusing on both the lower f–f and CT states. State-of-the-art quantum chemical methods will be applied. Before describing the theoretical methodology (the Computational Details section) and analyzing the computational results (the Computational Results and Discussion section), we briefly summarize the present understanding of the electronic structure of neptunyl(VI).

1.1. Model Concepts for Neptunyl(VI) Compounds. In order to understand chemical bonding, excited states, and absorption/emission spectra of neptunyl and its complexes, we refer to the axial-symmetric molecular orbitals (MOs) of bare neptunyl (see Figure 1). Under $D_{\infty h}$ symmetry, the Np 5f and

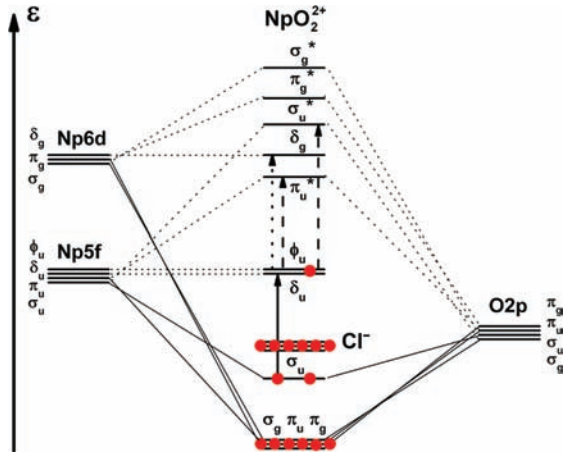

Figure 1. Qualitative scalar-relativistic valence orbital energy-level scheme for Np and O atoms on the left and right sides, and $D_{\infty h}$-neptunyl in the middle, the Cl-dominated MOs of $[NpO_2Cl_4]^{2-}$ being also indicated. The vertical solid arrow indicates the lowest electronic excitations of charge-transfer type (Np–O $2p\sigma_u \rightarrow$ Np $5f\delta_u,\phi_u$); the dashed and dotted arrows indicate ligand-field transitions of Np $5f\phi_u,\delta_u \rightarrow 5f\pi_u^*,\sigma_u^*$ and of Np $5f \rightarrow 6d\delta_g$ character, respectively.

6d atomic orbitals (AOs) transform as $f\sigma$, $f\pi$, $f\delta$, $f\phi$ and $d\sigma$, $d\pi$, $d\delta$, respectively. The electronic structure of NpO_2^{2+} is similar to that of closed-shell uranyl, except that an additional electron occupies a nonbonding orbital of Np 5f δ_u or ϕ_u type.[23,20] The O 2p lone-pair shells give rise to group orbitals of dative σ_u, σ_g, and pairs of π_u and π_g bonding type, which are stabilized by the Np $5f\sigma_u,\pi_u$ and Np $6d\sigma_g,\pi_g$ AOs. On the other hand, the Np 5f and 6d AOs of σ- and π-type mix into MOs, thereby gaining some antibonding character ($f\sigma_u^*$, $f\pi_u^*$, $d\sigma_g^*$, $d\pi_g^*$). Among the bonding MOs, σ_u is the least-stabilized one, because of the "push-from-below" orbital interaction of the Np $6p\sigma_u$ semicore AO, which is a mechanism well-known from the uranyl species.[24] The localized Np $5f\delta_u,\phi_u$- and $6d\delta_g$-type MOs are of nonbonding character and are labeled using AO notation. In $[NpO_2Cl_4]^{2-}$ with D_{4h} symmetry, the Cl lone-pair MOs reside 0.1–1.5 eV above the highest Np–O bonding MO, according to DFT calculations.

We are particularly interested in low-energy excitations and de-excitations. Therefore, we focus on the lowest excited states of f–f doublet type (absent in f^0-uranyl) and the ones of CT quartet type. An unpaired electron in the Np $5f\delta_u,\phi_u$ or $5f\pi_u^*,\sigma_u^*$ MOs of $[NpO_2]^{2+}$ and $[NpO_2Cl_4]^{2-}$ gives rise to low-lying $^2\Delta_u$ and $^2\Phi_u$ terms and higher-lying $^2\Pi_u$ and $^2\Sigma_u$ terms (dashed arrows in Figure 1), using $D_{\infty h}$ single-group symmetry labels. The Np $6d\delta_g$-type states (dotted arrow) are located in between.

The lowest CT transitions in neptunyl correspond to electron transfer from the highest occupied Np–O bonding σ_u MO to the nonbonding Np localized $5f\delta_u,\phi_u$-type MOs, indicated by the lower arrow in Figure 1. At the scalar-relativistic (SR) level, this gives rise to four quartet terms ($a^4\Sigma_u^-$, $b^4\Sigma_u^-$, $^4\Pi_u$, ^4H_u) and 10 doublet terms ($a^2\Sigma_u^+$, $b^2\Sigma_u^+$, $a^2\Sigma_u^-$, $b^2\Sigma_u^-$, $a^2\Pi_u$, $b^2\Pi_u$, $^2\Gamma_u$, a^2H_u, b^2H_u, ^2I_u), which are split by SO coupling (except the $^2\Sigma$ terms). The SO splitting scheme in $D_{\infty h}^*$ and D_{4h}^* double-group symmetry is displayed in Table 1. Remarkably, according

Table 1. Correlation of Symmetry Species of Point Groups $D_{\infty h}$ and D_{4h} and Respective Double Groups $D_{\infty h}^*$ and D_{4h}^*

$D_{\infty h}$	D_{4h}	$D_{\infty h}^*$	D_{4h}^*
$^2\Sigma_u^+$	$^2A_{2u}$	$E_{(1/2)u}$	$E_{(1/2)u}$
$^2\Pi_u$	^2E_u	$E_{(1/2)u} + E_{(3/2)u}$	$E_{(1/2)u} + E_{(3/2)u}$
$^2\Delta_u$	$^2B_{1u} + {}^2B_{2u}$	$E_{(3/2)u} + E_{(5/2)u}$	$2E_{(3/2)u}$
$^2\Phi_u$	^2E_u	$E_{(5/2)u} + E_{(7/2)u}$	$E_{(1/2)u} + E_{(3/2)u}$
$^4\Sigma_u^-$	$^4A_{1u}$	$E_{(1/2)u} + E_{(3/2)u}$	$E_{(1/2)u} + E_{(3/2)u}$
$^4\Pi_u$	^4E_u	$2E_{(1/2)u} + E_{(3/2)u} + E_{(5/2)u}$	$2E_{(1/2)u} + 2E_{(3/2)u}$
^4H_u	^4E_u	$E_{(7/2)u} + E_{(9/2)u} + E_{(11/2)u} + E_{13/2u}$	$2E_{(1/2)u} + 2E_{(3/2)u}$

to scalar relativistic CCSD(T) calculations the lowest Cl $\rightarrow$ Np CT state is 1.4 eV ($\sim 11 \times 10^3$ cm^{-1}) above the respective lowest Np–O σ_u CT state, contrary to the trend displayed in the MO energy levels (see Figure 1). This difference is not surprising as orbital energies reflect ionization energies, while excitation energies correspond to orbital energy differences plus significant two-electron energy terms. The comparatively high energy of the Cl $\rightarrow$ Np CT transition is due to the larger charge separation, as compared to the Np–O $\sigma_u \rightarrow$ Np CT transition.

2. COMPUTATIONAL DETAILS

Structures and spectra of NpO_2^{2+} and $NpO_2Cl_4^{2-}$ were investigated by using RASPT2[25] and CCSD(T)[26] approaches for electron correlation, as implemented in the MOLPRO 2008.1 program.[27] Cl and Np were represented by the Stuttgart energy-consistent relativistic effective core potentials (RECPs).[28] As well-documented in the literature,[29,30] the atomic (inner) cores are represented by frozen, relativistic, spin–orbit coupled, closed electron shells; the relativistic kinematics of the (outer core and) valence electrons is approximated by a nonrelativistic kinetic energy operator and a relativistic pseudo-potential operator, which simulates also the corrections due to relativistic kinematics, including spin–orbit coupling, in a Hilbert space of a pseudo-potential adapted valence orbital basis sets. The cores were chosen for Np as $1s^2$–$4f^{14}$ with SO-coupled 5spdf-6spd-7sp semicore and valence shells and for Cl as spin–orbit averaged $1s^22s^22p^6$ with a 3s3p valence shell. Here, the averaged spin–orbit coupling represents the so-called scalar relativistic approximation: the valence-shell spin–orbit splitting effects due to the Cl atoms are much smaller than reliably reproducible spin–orbit effects in the $NpO_2Cl_4^{2-}$ complex and may be safely neglected.

dx.doi.org/10.1021/ic202712p | Inorg. Chem. 2012, 51, 3231–3238

As is well-known,[29,30] relativistic pseudo-potentials combined with correlation consistent pseudo-potential basis sets[28] can be applied in various electron correlations (e.g., coupled clusters, multiconfiguration, and configuration interaction) approaches with reliable success, as is confirmed in recent literature.[21,31,32,38,39]

We have applied the aug-cc-pVDZ basis for O,[33] the ECP10MWB basis for Cl with an additional d-polarization function ($\zeta = 0.75$),[34] and the ECP60MWB-SEG basis for Np.[35,36] The low-lying doublet $5f^1$ and quartet CT ungerade states are listed in Table 2. The lowest doublet

Table 2. Valence Main-Configurations of Low Doublet f^1 Terms and Low Quartet CT Terms of NpO_2^{2+} in $D_{\infty h}$ Symmetry

term	main configuration(s)
$^2\Delta_u$	δ_u^1
$^2\Phi_u$	ϕ_u^1
$^4\Sigma_u^-$	$\sigma_u^1\delta_u^2$, $\sigma_u^1\phi_u^2$
^4H_u	$\sigma_u^1\delta_u^1\phi_u^1$
$^4\Pi_u$	$\sigma_u^1\delta_u^1\phi_u^1$

$6d^1$ gerade state was estimated to be at a much higher energy of ca. 42 500 cm^{-1}.[19] For simplicity, we will usually use the approximate $D_{\infty h}$ symmetry notations for the orbitals and states of $NpO_2Cl_4^{2-}$.

The geometries of the two lowest electronic single-reference states of $NpO_2Cl_4^{2-}$ were optimized by the CCSD(T) method, with convergence gradient criterion of $<1.0 \times 10^{-4}$. Born−Oppenheimer (BO) potential energies of the SO-averaged and SO-coupled excited states versus the Np−O distance were determined in steps of 1 pm and then fitted by polynomials, from which the Np−O equilibrium distances, vertical and adiabatic excitation energies and O−Np−O symmetric stretching frequencies were obtained. The error in the frequencies calculated by this approximation is estimated to be <2 cm^{-1}.[21]

2.1. Excited-State RASPT2 Calculations. The active spaces for the ground- and excited-state CASSCF calculations of NpO_2^{2+} and $NpO_2Cl_4^{2-}$ comprise the six bonding and six antibonding MOs of σ_u, σ_g, π_u, and π_g symmetry and Np 5f,6d/2O 2p character, and the four nonbonding Np 5f type orbitals of δ_u or ϕ_u symmetry (see Figure 1). This gives 13 electrons in 16 orbitals, denoted as CAS(13,16). Although single-point CASSCF calculations with such large spaces of configuration-state functions (CSFs) are feasible, subsequent CASPT2 calculations require excessive computer resources, particularly when scanning the potential energy curves point-wise. Therefore, somewhat configuration-restricted RASSCF calculations were performed.[37] Such an approach had yielded acceptable accuracies in the cases of UF_6,[38] UN_2, NUO^+, and UO_2^{2+},[39] and had been proven to be comparable to CASPT2/CASSCF/SO calculations of UO_2^{2+}.[40] In the case of the lower CT excitations of $NpO_2Cl_4^{2-}$, there is only very little Np ← Cl($\sigma\pi$) admixture, in contrast to predictions by the DFT approximation for all these cases. A similar defect of the TD-DFT approach in the case of $UO_2Cl_4^{2-}$ excitations and its electron detachments had been discussed by Pierloot et al.[40,41] and by us.[42] The common defects of orbital models for loosely bound transition-metal complexes have been explained by Buijse and Baerends.[43] Here, CAS(13,16) without the inclusion of halogen-localized MOs seems acceptable, as supported by some test calculations.

We have divided the active space into three subspaces: RAS1, RAS2, and RAS3. The six bonding orbitals with 12 electrons in the ground-state form RAS1; the four nonbonding orbitals with 1 electron in the ground-state form RAS2; and the six antibonding orbitals form RAS3. Excitations from RAS1 remain unrestricted, while only up to 2 electrons are allowed in RAS2 and up to 4 electrons in RAS3. The restriction scheme is denoted by S(2,4). Test calculations with the more-generous S(2,6) restriction have shown RAS-energy changes of 0.1 eV or less, but very little change at the RASPT2 level (<0.02 eV).

The computer time and memory use of the S(2,4) RASSCF and subsequent RASPT2 calculations is acceptable for NpO_2^{2+}. For $NpO_2Cl_4^{2-}$; however, it became too demanding, because of the additional Cl basis sets. Therefore, we allowed only 2 electrons in RAS3; i.e., we performed S(2,2) calculations on $NpO_2Cl_4^{2-}$. To evaluate the energy errors of this restriction, we also performed S(2,2) RASPT2 calculations on NpO_2^{2+}. The S(2,4)-S(2,2) changes in the range of up to 0.2 eV of the adiabatic excitation energies of NpO_2^{2+} were then added as corrections to the respective potential energy curves of $NpO_2Cl_4^{2-}$ and are labeled by S(2,4)/S(2,2).

State-averaged RASSCF calculations were carried out to generate the wave functions for the two doublet states ($^2\Delta_u$ and $^2\Phi_u$) simultaneously, or for the lower three quartet states ($a^4\Sigma_u^-$, $^4\Pi_u$, and ^4H_u).[44] RASPT2 calculations then were performed for each of those states of NpO_2^{2+} and $NpO_2Cl_4^{2-}$. In order to improve the RASPT2 convergence, level shifts were applied: 0.4 au for NpO_2^{2+} and 0.5 au for $NpO_2Cl_4^{2-}$, which were eventually removed near convergence.

SO coupling was taken into account by the state-interaction RAS-SI/SO approach.[45,46] The scalar-relativistic RASSCF wave functions of the electronic states in Table 2 were used to construct the respective complete 28 × 28 SO state interaction matrices, with the diagonal elements correlation-corrected using the RASPT2 energies.

2.2. Simulation of Luminescence Spectra. Following our previous work,[20,21] where the theoretical details are given, the ONPO-vibrational profiles of the luminescence spectra of the observed f−f transitions and the predicted CT transitions were modeled using the Franck−Condon formulas of Fonger and Struck.[47] They account for vibrational frequency changes upon electronic transition, but neglect anharmonicities and Duschinsky rotations, which are expected to be small for the cases at hand. In this paper, we only consider the symmetric stretching vibration of O−Np−O, neglecting the coupling with other vibration modes. The Np−O bond-length changes ΔR_{Np-O} of the luminescent states relative to the ground state are related to the Huang−Rhys factor S of the vibrational progression by $(\Delta R_{Np-O})^2 \approx S/(\omega_f m_O)$ (in au). ω_f is the final-state vibration frequency and m_O the atomic mass of the vibrating oxygen.[21] Note that this is without the sometimes-incorrectly applied factor of 2 before S.[20] Of course, the actual intensity pattern depends, in addition to S, on the initial to final vibration frequency ratio, the anharmonicity, and a vibration-dependent energy factor for absorption or emission.[20,23]

3. COMPUTATIONAL RESULTS AND DISCUSSION

3.1. SO-Averaged Results. The ground-state geometries of NpO_2^{2+} and $NpO_2Cl_4^{2-}$ were determined to have $D_{\infty h}$ and D_{4h} symmetry, respectively. The Np 5fϕ_u shell of NpO_2^{2+} remains degenerate as e_u under the D_{4h} symmetry of $NpO_2Cl_4^{2-}$, while the Np 5fδ_u shell is split into b_{1u} and b_{2u}, giving rise to two separate electronic doublet terms: $^2B_{1u}$ and $^2B_{2u}$. They were individually optimized by the single-reference CCSD(T) method, resulting in Np−Cl equilibrium distances of 267.61 and 268.36 pm, respectively. The $^2B_{1u}$ term with electron density maxima pointing toward the centers of the ClOCl triangle faces turned out to be the ground term, as to be expected, 0.13 eV below the $^2B_{2u}$. Accordingly, $R_{Np-Cl} = 267.61$ pm was chosen as the distance used for calculating all vertical excitation energies. This value for the anion in vacuum agrees reasonably with the experimental values of 265−267 pm for the $NpO_2Cl_4^{2-}$ units in crystals.[10,11,48] The Np−Cl distances increase slightly upon fδ_u to fϕ_u excitation (<1 pm), and a little more upon σ_u excitation (1−3 pm), indicating only weak Np−Cl bonding power of this basically Np−O bonding orbital. We note that the similar U−Cl bond length of $UO_2Cl_4^{2-}$ changes by only 1.4 pm[23] upon $\sigma_u \rightarrow$ U-5f$\delta_u\phi_u$ excitations, corroborated by the respective short progressions in the experimental spectra.[4] RASPT2 Born−Oppenheimer (BO) energy curves of the ground and low-lying excited states of NpO_2^{2+} and $NpO_2Cl_4^{2-}$ arising from the f→f and $\sigma_u \rightarrow \delta_u\phi_u$ excitations are displayed in Figure 2. Numerical data for

dx.doi.org/10.1021/ic202712p | Inorg. Chem. 2012, 51, 3231−3238

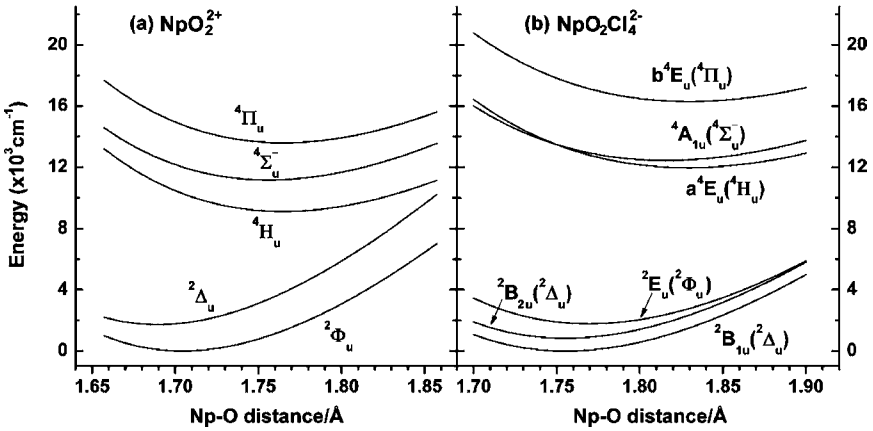

Figure 2. Energy curves of the ground and the low-lying excited terms of (a) NpO_2^{2+} and (b) $NpO_2Cl_4^{2-}$ for the O−Np−O symmetric stretch, at the scalar-relativistic level of RASPT2, calculations with restriction scheme S(2,2).

Table 3. Spectroscopic Data for NpO_2^{2+} and $NpO_2Cl_4^{2-}$ from Scalar Relativistic RASPT2 Calculations with Restriction Schemes S(2,4) and S(2,2)/S(2,4), Respectively[a]

NpO_2^{2+}				$NpO_2Cl_4^{2-}$			
term [$D_{\infty h}$]	R_e (pm)	T_e[b] (cm^{-1})	ν_s (cm^{-1})	term [$D_{4h}(D_{\infty h})$]	R_e (pm)	T_e[c] (cm^{-1})	ν_s (cm^{-1})
$^2\Phi_u$	171.0	0	911	$^2B_{1u}(^2\Delta_u)$	175.6	0	802
				$^2B_{2u}(^2\Delta_u)$	175.5	836	801
$^2\Delta_u$	169.4	1851 (128)	919	$^2E_u(^2\Phi_u)$	177.0	1651	801
^4H_u	176.6	10564 (1458)	746	$^4E_u(^4H_u)$	182.9	13301	663
$^4\Sigma_u^-$	175.7	12648 (935)	748	$^4A_{1u}(^4\Sigma_u^-)$	181.6	13800	679
$^4\Pi_u$	176.9	14522 (1483)	746	$^4E_u(^4\Pi_u)$	183.0	17097	663

[a] R_e = Np−O bond length; T_e = adiabatic excitation energy; and ν_s = O−Np−O symmetric stretching frequency. [b] S(2,4)/S(2,2); the correction of adiabatic excitation energy is given in parentheses. [c] Including the S(2,4)/S(2,2) correction of NpO_2^{2+}.

NpO_2^{2+} from scheme S(2,4) and for $NpO_2Cl_4^{2-}$ from scheme S(2,2) with the S(2,4)/S(2,2) correction are collected in Table 3.

Without SO coupling, because the Np 5fϕ_u AO is perturbed less by the O atoms than the Np 5fδu AO, the ground term of NpO_2^{2+} is (Np 5fϕ_u) $^2\Phi_u$, while the first excited term is (Np 5fδ_u) $^2\Delta_u$, as is also found in previous calculations on uranyl.[40,41,49,50] However, the equatorial Cl^- ligands in $NpO_2Cl_4^{2-}$ interact most strongly with the Np 5fϕ_u, because of direct orbital overlap, and shift it up from below to above the Np 5fδ_u level. This is consistent with the careful spectra analysis of Denning et al.,[8] who placed the 5fϕ_u ~1960 cm^{-1} (0.24 eV) above the 5fδ_u in the $Cs_2NpO_2Cl_4$ crystal. The quartet energy curves with strong 5fϕ_u contribution—$^4\Sigma_u^-$, ^4H_u, and $^4\Pi_u$—also are pushed up. This phenomenon has also been observed for uranyl and its complexes.[21,40,41,51] The push-up of ^4H_u and $^4\Pi_u$ is larger than that of $^4\Sigma_u^-$ by 1600 cm^{-1}, corresponding to ~50% 5fϕ_u contribution in ^4H_u and $^4\Pi_u$ versus only ~13% in $^4\Sigma_u^-$, which is again consistent with Denning's results. Finally, we note the ligand-field splitting of the $^2\Delta_u$ term of ~836 cm^{-1} in $NpO_2Cl_4^{2-}$.

On the average of all electronic states, the Np−O bond lengths are elongated by Cl^- coordination by ~6 ± 1 pm. Correspondingly, the symmetric stretching frequencies ν_s(ONpO) are reduced by ~115 cm^{-1} for the f-states, by 83 cm^{-1} for the ^4H_u and $^4\Pi_u$ CT states, and by 69 cm^{-1} for the $a^4\Sigma_u^-$ state, which has the least fϕ_u admixture. Both indicate a weakening of the neptunyl Np≡O triple bond by Lewis-base coordination in the equatorial plane of $NpO_2Cl_4^{2-}$. Similar trends have been observed in the case of uranyl complexes.[20,21,40,41,51]

The S(2,4)/S(2,2) corrections of the adiabatic excitation energies in Table 3 show only a small effect of the occupation restriction of the antibonding orbitals on the f-states (<200 cm^{-1}), while the restriction has an important impact on the CT states (~1000−1500 cm^{-1}).

3.2. Spin−Orbit Coupled Results. Several selected SO-coupled potential energy curves are presented in Figure 3. Numerical RASPT2 data of NpO_2^{2+} from scheme S(2,4), including also the higher CT states, are displayed and compared with literature data in Table 4. Our energies agree within ~10^3 cm^{-1} with Visscher's ones,[19] but deviate from Pitzer's[18] earlier ones by up to −3/+4 × 10^3 cm^{-1}. The results for $NpO_2Cl_4^{2-}$ are given in Table 5. For the two molecules, the SO splittings of the $^2\Delta_u$ terms are of the order of 4 × 10^3 cm^{-1}, and of the higher angular-momentum $^2\Phi_u$ terms at ~6 × 10^3 cm^{-1}, which is consistent with the atomic angular momentum model. Accordingly, with SO coupling, the ground state of $NpO_2Cl_4^{2-}$ has still-dominant $^2\Phi_u$ character with $\Omega = {}^5/_2$, being strongly mixed with $^2\Delta_{(5/2)u}$. Such mixing had already been deduced semiempirically by Denning et al. from the $Cs_2NpO_2Cl_4$ crystal spectra.[8]

The SO splittings of the ^4H_u terms are quite regular and are ~3000 cm^{-1}, with ${}^7/_2u$ below ${}^9/_2u$. Those of the $^4\Sigma_u^-$ (${}^1/_2u$) terms are ~1200 cm^{-1}. In both molecules, the lowest CT state has dominant ^4H_u character. The spin-averaged ^4H_u–$^4\Sigma_u^-$ separation is ~2000 cm^{-1} in NpO_2^{2+} and only ~500 cm^{-1} in $NpO_2Cl_4^{2-}$. The interplay of different ΛS splittings, different SO splittings, and the ligand-field splitting in $NpO_2Cl_4^{2-}$ leads to a near-degeneracy of the second and third CT terms in $NpO_2Cl_4^{2-}$, being dominated by ^4H_u and $^4\Sigma_u^-$ character,

dx.doi.org/10.1021/ic202712p | Inorg. Chem. 2012, 51, 3231−3238

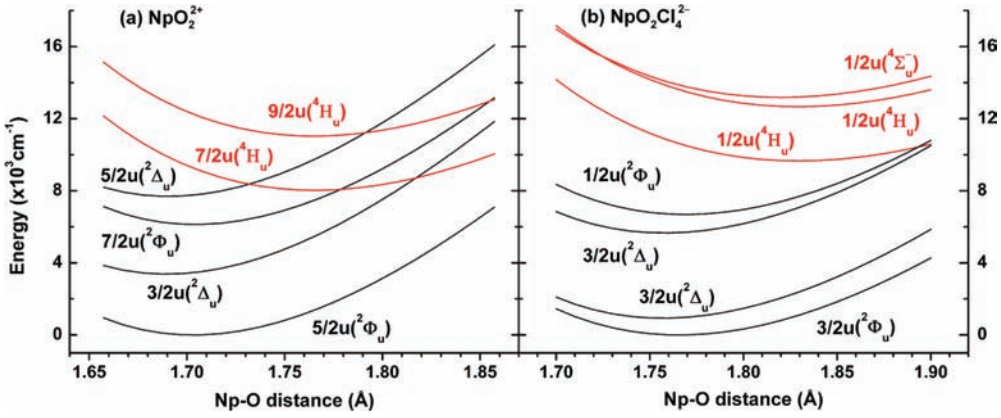

Figure 3. Energy curves of the ground and the low-lying excited terms of (a) NpO_2^{2+} and (b) $NpO_2Cl_4^{2-}$ for the O−Np−O symmetric stretch, at the SO coupled relativistic level of RASPT2 calculations with restriction scheme S(2,2). Red curves denote CT states, and black curves denote f-states. The SO-coupled electronic states are given in double-group notation with the corresponding ΛS states given in parentheses.

Table 4. NpO_2^{2+}: RASPT2/SO Results with Restriction Scheme S(2,4)[a]

		RASPT2/SO (this work)						SO-MRCI (ref 18)				IHFSCC (ref 19)
states	main term	%[b]	R_e (pm)	ΔR_e (pm)	E_v[c] (cm^{-1})	T_e (cm^{-1})	ν_s (cm^{-1})	R_e (pm)	ΔR_e (pm)	E_v[d] (cm^{-1})	ν_s (cm^{-1})	E_v[e] (cm^{-1})
$^5/_2u$	$^2\Phi_u$	91	170.8	0	0	0	908	165	0	0	1054	0
$^3/_2u$	$^2\Delta_u$	100	169.4	−1.4	3575	3503 (120)	919	164	−1	447	1058	3544
$^7/_2u$	$^2\Phi_u$	100	171.0	+0.2	6108	6107 (−30)	910	164	1	5515	1069	7227
$^5/_2u$	$^2\Delta_u$	90	169.5	−1.3	7861	7798 (102)	922	165	0	6565	1037	8929
$^7/_2u$	^4H_u	99	176.6	+5.8	10536	9498(1466)	747	170	+5	12622	874	
$^9/_2u$	^4H_u	100	176.6	+5.8	13520	12490(1450)	747			15418		
$^1/_2u$	$^4\Sigma_u^-$	61	176.3	+5.5	14712	13816(1187)	757			15668		
$^3/_2u$	$^4\Sigma_u^-$	75	176.1	+5.3	15841	15015(1301)	753			16664		
$^{11}/_2u$	^4H_u	100	176.7	+5.9	16503	15482(1434)	746			18676		
$^1/_2u$	$^4\Pi_u$	99	176.8	+6.0	18381	17282 (921)	746			21580		
$^{13}/_2u$	^4H_u	100	176.6	+5.8	19487	18475(1420)	745			21925		
$^5/_2u$	$^4\Pi_u$	100	176.9	+6.1	19963	18853 (908)	746			23882		
$^3/_2u$	$^4\Pi_u$	75	176.5	+5.7	20306	19318(1084)	741			22230		
$^1/_2u$	$^4\Pi_u$	62	176.3	+5.5	20584	19337 (866)	737			22469		

[a]See footnotes *a* and *b* of Table 3. [b]Percentage of the dominant "main term" in wave function. [c]Vertical transition at *R*(Np−O) = 170.7 pm. [d]Vertical transition at *R*(Np−O) = 166 pm. [e]Vertical transition at equilibrium bond distance of *R*(Np−O) = 170.1 pm.

Table 5. $NpO_2Cl_4^{2-}$: RASPT2/SO Results with Restriction Scheme S(2,2)/S(2,4)[a]

		$NpO_2Cl_4^{2-}$ RASPT2/SO (this work)					$Cs_2NpO_2Cl_4$ spectroscopic[b]		
state	main term	%	R_e (pm)	ΔR_e (pm)	T_e (cm^{-1})	ν_s (cm^{-1})	R_e (pm)	T_0 (cm^{-1})	ν_s (cm^{-1})
$^3/_2u$	$^2\Phi_u$	68	176.6	0	0	786	174.8, 177.5	0	802
$^3/_2u$	$^2\Delta_u$	88	175.7	−0.9	1055	812		∼1000	
$^3/_2u$	$^2\Delta_u$	79	175.8	−0.8	5767	809		6880	
$^1/_2u$	$^2\Phi_u$	100	176.9	+0.3	6658	800		7990	
$^1/_2u$	^4H_u	99	183.0	+6.4	11127	664		13265	722
$^1/_2u$	^4H_u	100	182.9	+6.3	14122	663		15683	711
$^1/_2u$	$^4\Sigma_u^-$	75	182.0	+5.4	14375	665		15406	715
$^3/_2u$	$^4\Sigma_u^-$	88	181.8	+5.2	15330	662		16800	713
$^3/_2u$	^4H_u	100	182.9	+6.3	17129	663			
$^1/_2u$	$^4\Pi_u$	99	183.0	+6.4	18774	663		19375	686
$^3/_2u$	^4H_u	100	182.9	+6.3	20134	661			
$^3/_2u$	$^4\Pi_u$	100	183.0	+6.4	20305	663			
$^1/_2u$	$^4\Pi_u$	77	182.6	+6.0	20372	658			
$^3/_2u$	$^4\Pi_u$	88	182.8	+6.2	20537	661			

[a]See footnotes *a* and *c* of Table 3 and footnote *b* of Table 4. [b]Experimental energy levels T_0 and ν_s(ONpO) of excited states come from refs 8 and 9; equilibrium bond length and ν_s(ONpO) of the ground state from ref 10.

dx.doi.org/10.1021/ic202712p | *Inorg. Chem.* 2012, 51, 3231−3238

respectively. In NpO_2^{2+}, they are still separated by 1300 cm^{-1}. The calculated and spectroscopically derived energy differences between these two terms of $NpO_2Cl_4^{2-}$ are +253 cm^{-1} and −280 cm^{-1}, which gives an indication of the reliability of our term values. One reason for the difference may be the neglect of higher CT excited states such as O-2pπ_u → Np 5f$\delta_w\phi_u$ in the SO−CI interaction matrix. As for bare neptunyl, the S(2,4)/S(2,2) corrections for $NpO_2Cl_4^{2-}$ are small for the f-states (∼100 cm^{-1}), but appreciable for the CT states (900−1500 cm^{-1}).

We stress the differences between bare NpO_2^{2+} (Table 4) and ligated $NpO_2Cl_4^{2-}$ (see Table 5), which is illustrated graphically in Figure 4. The order and the spacing of the state

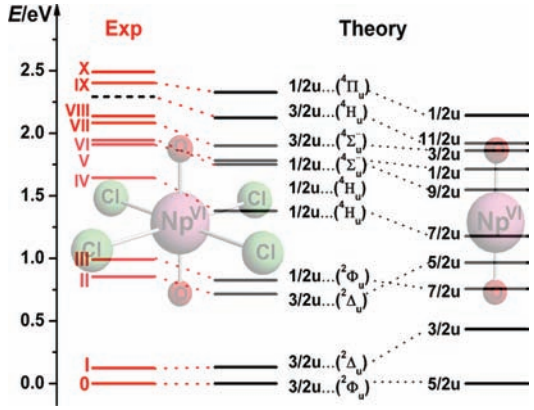

Figure 4. Comparison of electronic excitation energies from the experiment (red levels) of $Cs_2NpO_2Cl_4$ crystal and theoretical calculations (black levels) for $NpO_2Cl_4^{2-}$ and NpO_2^{2+} ions with different slopes of the lines connecting the ligated and nonligated neptunyl.

energies are different for the two species. The lowest f−f transition energy decreases from 3.5 × 10^3 cm^{-1} to 1.0 × 10^3 cm^{-1}, in excellent agreement with the experimental results for crystalline [$Cs_2NpO_2Cl_4$]. The calculated R_e(Np−O) and ν_s(ONpO) for the ground state of the $NpO_2Cl_4^{2-}$ building block also agree well with the experimental data for [$Cs_2NpO_2Cl_4$], with a difference of 2 pm for R_e(Np−O) and of 16 cm^{-1} for ν_s. The calculated results for the CT states differ more from the experimental crystal data (our T_e values are low by (1−2) × 10^3 cm^{-1}, the ν_s values are low by ∼60 cm^{-1}). As mentioned, our Np−O ground-state equilibrium distance of $NpO_2Cl_4^{2-}$ agrees reasonably well with the crystal structure values of [$Cs_2NpO_2Cl_4$],[10] while Pitzer's value for NpO_2^{2+} is lower than ours by 5−6 pm.

3.3. Luminescence of $NpO_2Cl_4^{2-}$. Luminescence of Np(VI) f−f transitions in the 6000−7000 cm^{-1} IR region with the origin at 6880 cm^{-1} has been observed at room temperature (and liquid nitrogen temperature). In the solid,[10,11] hot bands of $NpCl_4$ out-of-plane (117 cm^{-1}) and ONpO bending (267 cm^{-1}) vibrations, and very weak, short progressions of just single bands of the $NpCl_4$ out-of-plane, ONpO bending and symmetric stretching (802 cm^{-1}) vibrations were observed with lifetimes of a few tens of microseconds. In solution,[13] the transitions are quenched due to hydrogen-bond interactions, the lifetimes decrease by 3 orders of magnitude or more. Through high-resolution absorption spectroscopy, Denning[8] had already deduced negligible changes of Np−O bonding upon this f−f transition. This agrees with our finding of a symmetric bond-length reduction of ΔR_e(Np−O) upon fδ−fϕ transition of <1 pm (see Table 5).

Because of the significant SO coupling around the Np nucleus, rapid internal energy transfer from the higher CT quartet states to the lower f doublet states is to be expected, in particular in solution.[13] If emission from the lowest quartet state becomes detectable, a remarkable progression of the O−Np−O symmetric stretching mode is expected, corresponding to the calculated bond-length expansion of ΔR_e(Np−O) = 6.4 pm, and consistent with the absorption spectra.[9]

Figure 5 presents the simulated luminescence progressions of the symmetric O−Np−O stretching mode for the observed f−f and the predicted CT emissions. The respective numerical parameters for the simulation are displayed in Table 6. Since

Table 6. Parameters for Luminescence Spectra Simulation of $NpO_2Cl_4^{2-}$[a]

term	ΔR_e (pm)	T_0 (cm^{-1})	$\nu_{s,g}$ (cm^{-1})	$\nu_{s,e}$ (cm^{-1})	Γ (cm^{-1})
$^3/_2u$ ($^2\Delta_u$)	−0.8	6880	786	809	63
$^1/_2u$ (^4H_u)	+6.4	13265	786	664	63

[a] $\nu_{s,g}$ and $\nu_{s,e}$ are the symmetric stretching frequencies of the ground state and the luminescent state; see footnote *a* of Table 3 for ΔR_e and footnote *b* of Table 5 for T_0.

the present state-of-the-art does not yield spectroscopically accurate adiabatic excitation energies (or term values), nor reasonable estimations for the homogeneous and heterogeneous line broadenings, we use the experimental T_0 values of $Cs_2NpO_2Cl_4$ and the Γ value of UO_2Cl_2.[21]

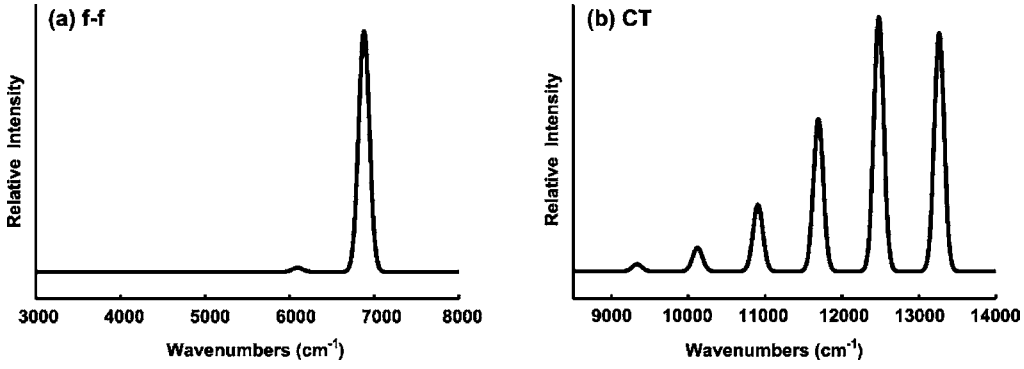

Figure 5. Simulated low-temperature luminescence spectrum of (a) the second-lowest f−f and (b) the lowest charge-transfer (CT) excited state of $NpO_2Cl_4^{2-}$.

dx.doi.org/10.1021/ic202712p | Inorg. Chem. 2012, 51, 3231−3238

4. CONCLUSIONS

We have investigated the electronic spectra and some luminescence properties of low-lying f−f and charge-transfer (CT) ($\sigma_u \rightarrow \delta_u, \phi_u$) transitions of NpO_2^{2+} and $NpO_2Cl_4^{2-}$, applying a relativistic ECP-based RASSCF/RASPT2/SO approach with two different configuration-restriction schemes. Restricting the occupation number of Np−O antibonding orbitals has little influence on the f-f transition energies (<200 cm^{-1}), but is important for the CT states with an open shell of bonding MOs (up to 1500 cm^{-1}). The present study improves on previous calculations of excited neptunyl states.[18] Among others, we predict the so-far unobserved $^3/_2u$ ($^4H_{(11/2)u}$) CT term at (18.5−19.0) × 10^3 cm^{-1}, between terms VIII and IX, observed/calculated at 16.8 × 10^3 cm^{-1}/15.3 × 10^3 cm^{-1} and 19.4 × 10^3 cm^{-1}/18.8 × 10^3 cm^{-1}, respectively. The semiempirical ligand-field model of Denning places it ∼2000 cm^{-1} higher, i.e., at 20.7 × 10^3 cm^{-1}. Yet, because RASPT2 is an efficient, although not the most accurate, multireference ab initio method,[52] there is room for future improvement by applying more-advanced electron correlation techniques (e.g., MR-CISD or r_{12}-based methods) with more-complete atomic basis sets and larger configuration spaces including the ligands.

The calculated lowest f−f transition energy of $NpO_2Cl_4^{2-}$ reproduces the experimental value of the [$Cs_2NpO_2Cl_4$] crystal within 100 cm^{-1}. Concerning all higher doublet f−f and quartet CT states, the calculated excitation energies for $NpO_2Cl_4^{2-}$ in vacuum are smaller than the experimental ones for the Cs salt crystal. There are significant differences in the energy values and order between bare NpO_2^{2+} and ligated $NpO_2Cl_4^{2-}$, as shown in Figure 4. Therefore, it is not advisible to assign the spectra of neptunyl complex compounds on the basis of the free neptunyl ion. Our improved theoretical spectral assignment supports and extends Denning's earlier empirical ones.[8,9]

We find very weak vibronic transitions of the O−Np−O symmetric stretching mode accompanying the f−f transitions, which is consistent with the experimental observations.[8,10,11,13] The vibronic symmetric ONpO stretching progression in the possible luminescence from the lowest CT state has been predicted.

AUTHOR INFORMATION

Corresponding Author

*E-mail: junli@mail.tsinghua.edu.cn.

Present Address

†Physical and Theoretical Chemistry, University of Siegen, 57068 Siegen, Germany (E-mail: eugen.schwarz@uni-siegen.de).

Notes

The authors declare no competing financial interest.

ACKNOWLEDGMENTS

This work was financially supported by NSFC (Nos. 20933003, 11079006, 91026003) of China. The calculations were performed by using computers at the Supercomputer Center of the Computer Network Information Center, Chinese Academy of Sciences, and at the Shanghai Supercomputing Center. A portion of the calculations was performed using EMSL, a national scientific user facility sponsored by the U.S. Department of Energy's Office of Biological and Environmental Research and located at the Pacific Northwest National Laboratory, USA.

REFERENCES

(1) Yoshida, Z.; Johnson, S. G.; Kimura, T.; Krsul, J. R. *The Chemistry of the Actinide and Transactinide Elements*, 4th Edition; Morss, L. R., Edelstein, N. M., Fuger, J., Eds; Springer: Berlin, New York, 2011; Chapter 6, pp 699−812 (DOI: 10.1007/978-94-007-0211-0_6).

(2) Rabinowitch, E.; Belford, R. L. *Spectroscopy and Photochemistry of Uranyl Compounds*; Oxford University Press: Oxford, U.K., 1964.

(3) Denning, R. G.; Snellgrove, T. R.; Woodwark, D. R. *Mol. Phys.* **1976**, *32*, 419−442.

(4) Barker, T. J.; Denning, R. G.; Thorne, J. R. G. *Inorg. Chem.* **1987**, *26*, 1721−1732.

(5) Flint, C. D.; Tanner, P. A. *J. Chem. Soc. Faraday Trans. II* **1978**, *74*, 2210−2217.

(6) Barker, T. J.; Denning, R. G.; Thorne, J. R. G. *Inorg. Chem.* **1992**, *31*, 1344−1353.

(7) Denning., R. G. *Struct. Bonding (Berlin)* **1992**, *79*, 215−276.

(8) Denning, R. G.; Norris, J. O. W.; Brown, D. *Mol. Phys.* **1982**, *46*, 287−323.

(9) Denning, R. G.; Norris, J. O. W.; Brown, D. *Mol. Phys.* **1982**, *46*, 325−364.

(10) Wilkerson, M. P. *J. Chem. Crystallogr.* **2004**, *34*, 807−811.

(11) Wilkerson, M. P.; Arrington, C. A.; Berg, J. M.; Scott, B. L. *J. Alloys Compd.* **2007**, *444−445*, 634−639.

(12) Wilkerson, M. P.; Berg, J. M.; Hopkins, T. A.; Dewey, H. J. *J. Solid State Chem.* **2005**, *178*, 584−588.

(13) Talbot-Eeckelaers, C.; Pope, S. J. A.; Hynes, A. J.; Copping, R.; Jones, C. J.; Taylor, R. J.; Faulkner, S.; Sykes, D.; Livens, F. R.; May, I. *J. Am. Chem. Soc.* **2007**, *129*, 2442−2443.

(14) Eisenstein, J. C.; Pryce, M. H. L. *J. Res. Natl. Bur. Stand. A* **1965**, *69*, 217−227.

(15) Pershina, V. G.; Ionova, G. V.; Suraeva, N. I. *Russ. J. Inorg. Chem.* **1990**, *35*, 1178−1181.

(16) Makhyoun, M. A. *Inorg. Chem.* **1987**, *26*, 3592−3595.

(17) Li, J; Bursten, B. E. *J. Am. Chem. Soc.* **1998**, *120*, 11456−11466.

(18) Matsika, S.; Pitzer, R. M. *J. Phys. Chem. A* **2000**, *104*, 4064−4068.

(19) Infante, I.; Gomes, A. S. P.; Visscher, L. *J. Chem. Phys.* **2006**, *125*, 074301.

(20) Su, J.; Zhang, K.; Schwarz, W. H. E.; Li, J. *Inorg. Chem.* **2011**, *50*, 2082−2093.

(21) Su, J.; Wang, Y. L.; Wei, F.; Schwarz, W. H. E.; Li, J. *J. Chem. Theory Comput.* **2011**, *7*, 3293−3303.

(22) Su, J.; Li, J. *Prog. Chem.* **2011**, *23*, 1329−1337.

(23) Denning, R. G. *J. Phys. Chem. A* **2007**, *111*, 4125−4143.

(24) Pepper, M.; Bursten, B. E. *Chem. Rev.* **1991**, *91*, 719−741.

(25) Malmqvist, P.-Å.; Pierloot, K.; Shahi, A. R. M.; Cramer, C. J.; Gagliardi, L. *J. Chem. Phys.* **2008**, *128*, 204109.

(26) Raghavachari, K.; Trucks, G. W.; Pople, J. A.; Head-Gordon, M. *Chem. Phys. Lett.* **1989**, *157*, 479.

(27) Werner, H.-J.; Knowles, P. J.; Lindh, R.; Manby, F. R.; Schütz, M.; Celani, P.; Korona, T.; Mitrushenkov, A.; Rauhut, G.; Adler, T. B.; Amos, R. D.; Bernhardsson, A.; Berning, A.; Cooper, D. L.; Deegan, M. J. O.; Dobbyn, A. J.; Eckert, F.; Goll, E.; Hampel, C.; Hetzer, G.; Hrenar, T.; Knizia, G.; Koppl, C.; Liu, Y.; Lloyd, A. W.; Mata, R. A.; May, A. J.; McNicholas, S. J.; Meyer, W.; Mura, M. E.; Nicklass, A.; Palmieri, P.; Pflüger, K.; Pitzer, R.; Reiher, M.; Schumann, U.; Stoll, H.; Stone, A. J.; Tarroni, R.; Thorsteinsson, T.; Wang, M.; Wolf, A. MOLPRO, version 2008.1, a package of *ab initio* programs; University College Cardiff Consultants Limited: Wales, U.K., 2008 (see http://www.molpro.net).

(28) Nicklass, A.; Dolg, M.; Stoll, H.; Preuß, H. *J. Chem. Phys.* **1995**, *102*, 8942−8952, http://www.theochem.uni-stuttgart.de/pseudopotentials.

(29) Schwarz, W. H. E. *Theor. Chim. Acta* **1968**, *11*, 307−324. Schwarz, W. H. E. *Theor. Chim. Acta* **1971**, *23*, 147−154. Chang, T. C.; Habitz, P.; Pittel, B.; Schwarz, W. H. E. *Theor. Chim. Acta* **1974**, *34*, 263−275. Hafner, P.; Schwarz, W. H. E. *J. Phys. B Atom. Mol. Phys.* **1978**, *11*, 217−233. Hafner, P.; Schwarz, W. H. E. *J. Phys. B Atom. Mol. Phys.***1978**, *11*, 2975−2999.

(30) Schwarz, W. H. E. *Relativistic Methods for Chemists*; Barysz, M., Ishikawa, Y., Eds.; Springer: Dordrecht, The Netherlands, 2010; pp 1−62.
(31) Wang, X.-B.; Wang, Y.-L.; Yang, J.; Xing, X.-P.; Li, J.; Wang, L.-S. *J. Am. Chem. Soc.* **2009**, *131*, 16369−16370.
(32) Liu, H.-T.; Xiong, X. G.; Dau, P. D.; Wang, Y.-L.; Li, J.; Wang, L.-S. *Chem. Sci.* **2011**, *2*, 2101−2108.
(33) Dunning, T. H. *J. Chem. Phys.* **1989**, *90*, 1007−1023.
(34) Bergner, A.; Dolg, M.; Kuechle, W.; Stoll, H.; Preuss, H. *Mol. Phys.* **1993**, *80*, 1431.
(35) Cao, X.; Dolg, M.; Stoll, H. *J. Chem. Phys.* **2003**, *118*, 487.
(36) Cao, X.; Dolg, M. *J. Mol. Struct. (Theochem)* **2004**, *673*, 203.
(37) Olsen, J.; Roos, B. O.; Jørgensen, P.; Jensen, H. J. A. *J. Chem. Phys.* **1988**, *89*, 2185−2192.
(38) Wei, F.; Wu, G. S.; Schwarz, W. H. E.; Li, J. *J. Chem. Theory Comput.* **2011**, *7*, 3223−3231.
(39) Wei, F.; Wu, G. S.; Schwarz, W. H. E.; Li, J. *Theor. Chem. Acc.* **2011**, *129*, 467−481.
(40) Pierloot, K.; van Besien, E. *J. Chem. Phys.* **2005**, *123*, 204309.
(41) Pierloot, K.; van Besien, E.; van Lenthe, E.; Baerends, E. J. *J. Chem. Phys.* **2007**, *126*, 194311.
(42) Dau, P. D.; Su, J.; Liu, H. T.; Liu, J. B; Huang, D. L.; Li, J.; Wang., L. S. *Chem. Sci.* **2012**, DOI: 10.1039/c2sc01052f.
(43) Buijse, M. A.; Baerends, E. J. *J. Chem. Phys.* **1990**, *93*, 4129−4141.
(44) Scalar relativistic CCSD(T) calculation shows that the $b^4\Sigma_u^-$ state is higher than the $a^4\Sigma_u^-$ state by 9000 cm^{-1}.
(45) Malmqvist, P. Å.; Roos, B. O.; Schimmelpfennig, B. *Chem. Phys. Lett.* **2002**, *357*, 230−240.
(46) Roos, B. O.; Malmqvist, P. Å. *Phys. Chem. Chem. Phys.* **2004**, *6*, 2919−2927.
(47) Fonger, W. H.; Struck, C. W. *J. Chem. Phys.* **1974**, *60*, 1994−2002.
(48) Cornet, S. M.; Redmond, M. P.; Collison, D.; Sharrad, C. A.; Helliwell, M.; Warren, J. *C. R. Chim.* **2010**, *13*, 832−838.
(49) Réal, F.; Vallet, V.; Marian, C.; Wahlgren, U. *J. Chem. Phys.* **2007**, *127*, 214302.
(50) Réal, F.; Gomes, A. S. P.; Visscher, L.; Vallet, V.; Eliav, E. *J. Phys. Chem. A* **2009**, *113*, 12504−12511.
(51) Wang, Q.; Pitzer, R. M. *J. Phys. Chem. A* **2001**, *105*, 8370−8375.
(52) Vancoillie, S.; Zhao, H.; Tran, V. T.; Hendrickx, M. F. A.; Pierloot, K. *J. Chem. Theory Comput.* **2011**, *7*, 3961−3977.